14.2.2 Auger Electron Spectroscopy

The process on which AES is based is similar to that of XPS, but it is a two-step process instead of one step. As with XPS, the sample is irradiated with either accelerated electrons or X-ray photons. An inner shell electron is ejected, leaving a vacancy in the inner shell. An electron from an outer shell falls into the inner shell as in the XPS process. The ion then either emits an X-ray photon

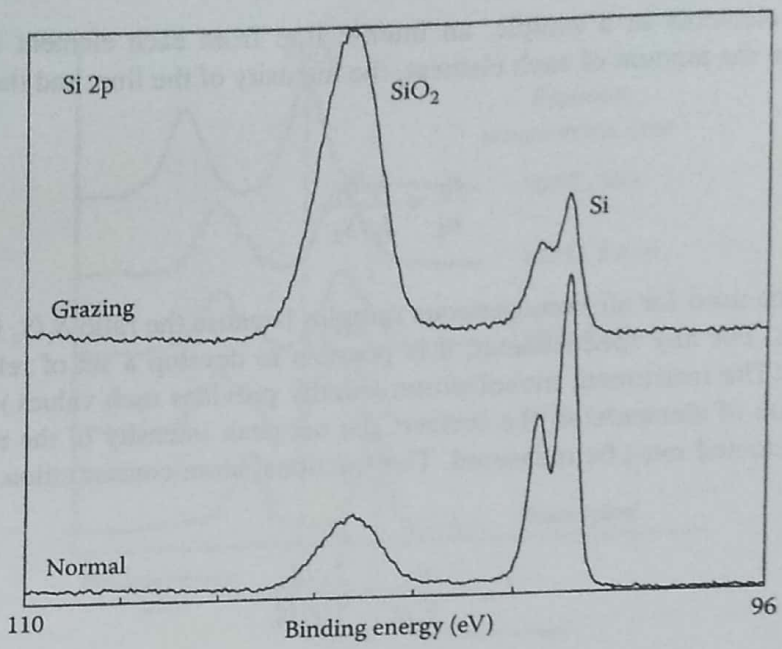

Figure 14.20 An example of the enhanced surface sensitivity achieved by varying the electron take-off angle. A thin SiO_2 oxide layer on silicon (Si) is enhanced at the shallow grazing angle. (From Moulder, J.F. et al., In *Handbook of X-Ray Photoelectron Spectroscopy*, Chastian, J. and King, R.C., eds., Physical Electronics, Inc., Eden Prairie, MN, 1995; Courtesy of Physical Electronics, Inc., Eden Prairie, MN, www.phi.com.)

or an Auger electron. In X-ray emission, the energy balance is maintained by the emission of an X-ray photon with energy equal to the difference between the two energy levels involved (Figure 14.1). This is XRF, discussed in Chapter 8. In the Auger process, the released energy is transferred to a second electron in an outer shell, which is then emitted. This is the Auger electron. The actual process by which the energy is transferred is not clearly understood but can be represented schematically as in Figures 14.2 and 14.21.

In the examples in both figures, an electron from the K shell was ejected by bombardment. An electron from the L shell descended to the K shell, simultaneously transferring energy to a second

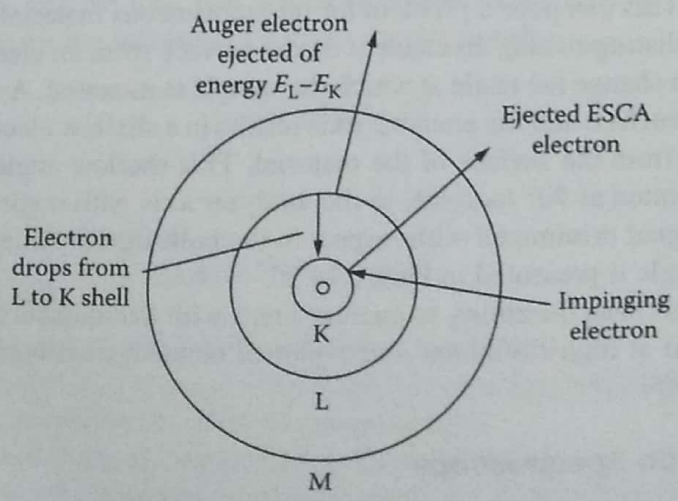

Figure 14.21 A simplified view of the process of Auger electron emission. An impinging electron ejects an inner shell electron, leaving an incomplete K shell. An electron from the L shell drops into the K shell, and simultaneously, an Auger electron is emitted from the L shell with energy $E_L - E_K$. This process competes with the process that produces X-ray photons (XRF) shown in Figure 14.1.

electron in the L shell. This second electron was ejected as an Auger electron. This Auger electron is termed a KLL Auger electron. This nomenclature arises from the fact that an electron was ejected from a K shell followed by a transition from an L to a K shell, simultaneously liberating an L Auger electron. It can be deduced that other Auger transitions, such as LMM and MNN, are also possible.

The Auger electron is ejected by the energy released by relaxation, that is, by the neighboring electron that drops into the inner orbital. The energy released on relaxation is a function of the particular atom and not of the energy of the source used to eject the initial electron from the inner orbital. Therefore, the kinetic energy of the Auger electron is independent of the energy range of the radiation source falling on the sample. This means that the source does not have to be monoenergetic (or monochromatic). Because the Auger peaks are independent of the source energy, unlike the XPS peaks, they can be distinguished readily from the XPS peaks. When spectra are collected with two different source energies, as shown in Figures 14.9 and 14.10, the binding energy of the Auger electron apparently changes with source energy, while the binding energies of the XPS photoelectrons do not.

The Auger process and XRF are competitive processes for the liberation of energy from bombarded atoms. In practice, it is found that the Auger process is more likely to occur with low atomic number elements; this probability decreases with increasing atomic number. In contrast, XRF is unlikely with elements of low atomic number but increases in probability with increasing atomic number. This is illustrated in Figure 14.22. The energies involved in Auger spectroscopy are similar in all respects to those of XPS, since the same atomic shells are involved. A graphical plot of Auger electron energies is shown in Figure 14.23, and tabulated values of the prominent lines are available in the literature.

AES is an elemental surface analysis technique that can detect elements from lithium to uranium with a sensitivity of about 0.5 atom%. Auger spectra consist of a few peaks for each element in the same energy region, 0–1000 eV, as XPS peaks. Auger peaks are less intense than XPS peaks as seen in Figures 14.9 and 14.12. Therefore, Auger spectra are generally plotted as the first derivative of the signal, $dN(E)/dE$, vs. the Auger electron energy (Figure 14.24). The use of the first derivative of the signal is a common practice to enhance small signals and to minimize the high and sloping background from scattered electrons.

Auger chemical shift: The chemical environment of the atom also shifts the Auger lines in the same way the XPS lines are shifted. The chemical shift magnitude may be greater for the Auger lines than for the XPS chemical shift. The Auger chemical shift is very useful for the identification of chemical states. A plot of Auger electron kinetic energy vs. the XPS photoelectron binding energy is a useful tool for identifying the chemical states of an element. We can define a quantity

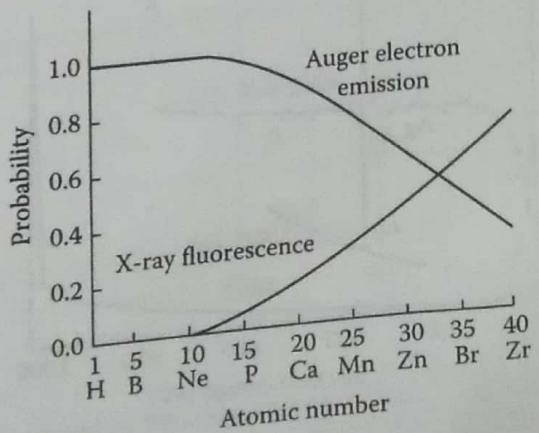

Figure 14.22 Relationship between atomic number and the probabilities of XRF and Auger electron emission. (Reprinted with permission from Hercules, D.M., *Anal. Chem.*, 42(1), 20A, 1970. Copyright 1970 American Chemical Society.)

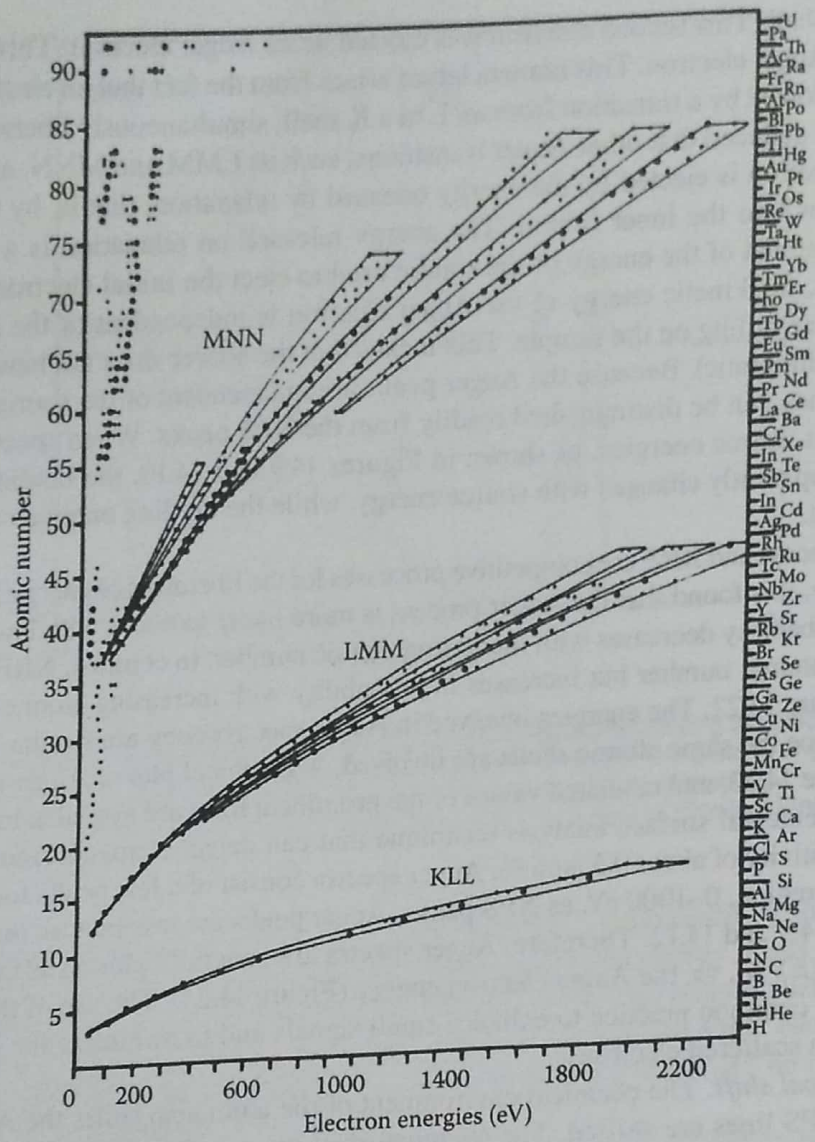

Figure 14.23 Principal Auger electron energies. (Courtesy of Physical Electronics, Inc., Eden Prairie, MN, www.phi.com.)

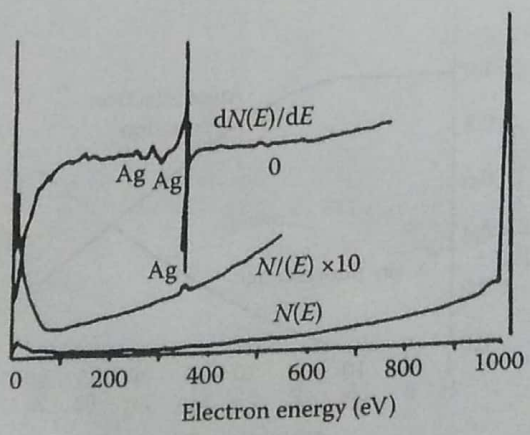

Figure 14.24 The direct Auger spectrum of silver (bottom), the direct spectrum with a 10-fold enhancement of the signal (middle), and the derivative or differential spectrum (top). The derivative spectrum significantly improves the ability to measure a small signal against a high and sloping background signal. (From Weber, R.E., *Res. Dev.*, 10, 22, 1972.)

called the Auger parameter as the difference between the kinetic energies of the Auger electron and the photoelectron:

$$AP = KE_{(A)} - KE_{(P)} = BE_{(P)} - BE_{(A)} \tag{14.8}$$

where
AP is the Auger parameter
$KE_{(A)}$ and $KE_{(P)}$ are the kinetic energy of the Auger electron (A) and photoelectron (P), respectively
BE is the binding energy of the respective electrons

It can be shown that

$$KE_{(P)} = h\nu - BE_{(A)}$$

that leads to

$$KE_{(A)} + BE_{(P)} = AP + h\nu \tag{14.9}$$

Plots of $KE_{(A)}$ vs. $BE_{(P)}$, with $AP + h\nu$ shown on the other ordinate (called Wagner plots) are found in the literature and in the NIST XPS database. An example for tin is presented in Figure 14.25. The Sn $3d_{5/2}$ photoelectron and the Sn MNN Auger electron binding energies are tabulated and

Tin		
Compound	Sn $3d_{5/2}$ Binding energy (eV)	Sn MNN Kinetic energy (eV)
Sn	484.9	437.4
Sn	485.0	437.4
Sn	485.1	437.4
SnS	485.6	435.7
Na_2SnO_3	486.2	431.7
SnO_2	486.7	432.7
Na_2SnO_3	486.7	431.7
Na_2SnO_3	487.2	431.7
$NaSnF_3$	487.4	430.8

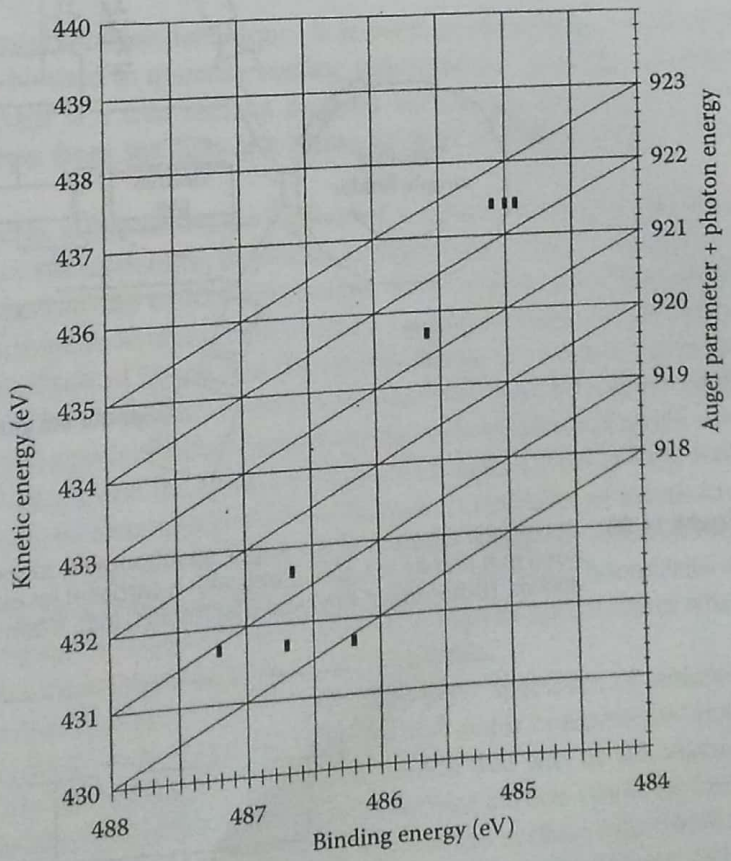

Figure 14.25 Table of values and plot of the Auger MNN electron kinetic energy for tin and Auger parameter vs. the photoelectron binding energy for the tin $3d_{5/2}$ electron in the element and a variety of compounds. The metal and different chemical states of tin in compounds can be readily distinguished. (From Moulder, J.F. et al., In *Handbook of X-Ray Photoelectron Spectroscopy*, Chastian, J. and King, R.C., eds., Physical Electronics, Inc., Eden Prairie, MN, 1995; Courtesy of Physical Electronics, Inc., Eden Prairie, MN, www.phi.com.)

plotted for the element Sn and a variety of tin compounds, showing how the chemical environment of the Sn affects the electron energies.

14.2.2.1 Instrumentation for AES

The instrumentation used in AES is very similar to that used in XPS. The major difference is that the source used is a focused beam of electrons from an electron gun or a field emission source, not X-ray photons. A schematic diagram of an AES instrument is shown in Figure 14.26. Many instrument manufacturers provide instruments that permit both XPS and Auger spectra to be collected on one instrument.

The advantage of an electron beam is that it can be focused and deflected. The electron beam can be focused, depending on the source, from a spot size of 10 nm to a spot size of several hundred micrometers. The focused beam can be scanned over the surface. This permits compositional mapping of a surface with very high resolution and the ability to study very small features. Electron guns may use a heated tungsten filament or lanthanum hexaboride rods as the cathode. Figure 14.27 shows a schematic cross section of an electron gun with a tungsten filament.

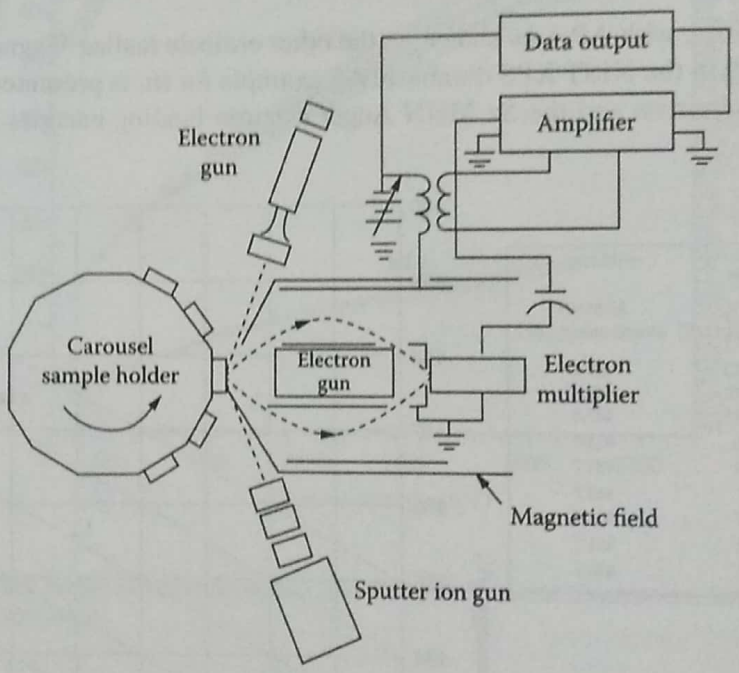

Figure 14.26 Schematic diagram of an Auger spectrometer, showing the electron gun source, an electron flood gun and an ion gun, along with a carousel for multiple samples. The vacuum system is not shown. (Courtesy of Physical Electronics, Inc., Eden Prairie, MN, www.phi.com.)

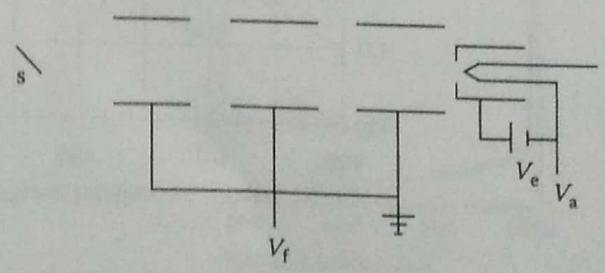

Figure 14.27 A schematic cross section of an electron gun with a tungsten filament and an Einzel lens focusing arrangement. S is the sample, V_f is the focus voltage, V_e is the emission voltage, and V_a is the acceleration voltage. (From Turner, N.H., Electron spectroscopy, in Ewing, G.W., ed., *Analytical Instrumentation Handbook*, 2nd edn., Marcel Dekker, Inc., New York, 1997. With permission.)

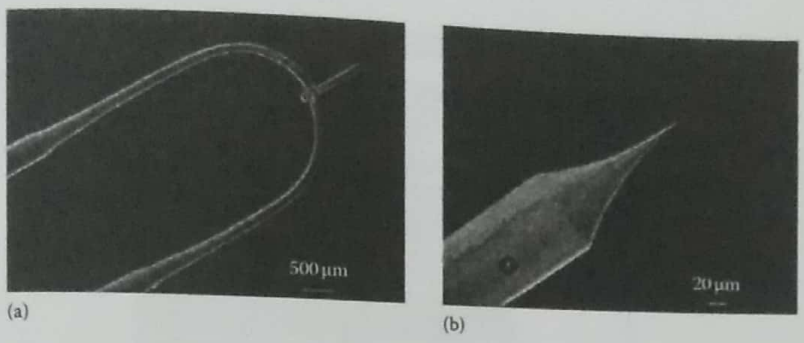

Figure 14.28 Field emitter of single-crystal tungsten is shown (a) on its supporting hairpin and (b) in a close-up view of the tip. (From Stinger, K., *Res. Dev.*, 28(9), 40, 1977.)

A field emission source uses a needle-like tungsten or carbon tip as the cathode, shown in Figure 14.28. The tip is only nanometers wide, resulting in a very high electric field at the tip. Electrons can tunnel out of the tip with no input of thermal energy, resulting in an extremely narrow beam of electrons. Electron beams from heated filaments have a focal (crossover) diameter of about 50 µm, while a field emission source has a crossover diameter of only about 10 nm. Field emission sources can serve as probes of surfaces at the nanometer scale (an Auger nanoprobe).

14.2.2.2 Applications of AES

AES is primarily a surface elemental analysis technique. It is used to identify the elemental composition of solid surfaces and can be used to quantify surface components, although quantitative analysis is not straightforward. AES is a true surface analysis technique, because the low-energy Auger electrons can only escape from the first few (three to five) atomic layers or from depths of 0.2 to 2.0 nm.

The electron beam can be deflected in a line across the surface of a sample to analyze multiple points or it can be rastered (moved in two dimensions) to produce a compositional map of the surface. Very small spot size and large magnifications (up to 20,000×) enable AES to study extremely small particles and intricate structures such as those used in microelectronics. Depth profiling with ion beam sputtering of the surface permits the analysis of layers and the identification of components in the grain boundaries of crystalline materials. The use of AES to study segregation of impurities in the grain boundaries of metals and alloys has played a pivotal role in understanding embrittlement of steels, corrosion and stress corrosion cracking of alloys, and the behavior of ductile tungsten used in light bulb filaments. Very often, sulfur, phosphorous, or carbon impurities in the grain boundaries of metals and alloys are the sites at which corrosion, cracking, and failure of the alloy are initiated. Alternatively, impurities in the grain boundaries may have a beneficial effect. Potassium in the grain boundaries of ductile tungsten acts as a lubricant, allowing the tungsten wire filament to expand and contract when a light bulb is switched on and off without breaking along the grain boundaries.

Some application examples are presented. Figure 14.29 shows the Auger spectrum of stainless steel before and after heating at 750°C for 10 min. It can be seen that the major components, iron, nickel, and chromium, are unchanged by the heating. However, the carbon that was on the surface of the stainless steel before heating disappeared after heating. This surface carbon could be from traces of lubricating oil or cutting fluid, for example. Sulfur is present on the surface after heating and the phosphorus signal has increased. This may be due to diffusion from the bulk stainless steel to the surface during heating.

The electron beam can scan a surface area systematically in what is called a raster scan. By monitoring the intensity of the Auger spectrum of a particular element during scanning, it is possible to map its distribution on the surface examined. An example of this technique is shown in Figure 14.30, which reveals the concentrations and location of sulfur and nickel on a spent catalyst

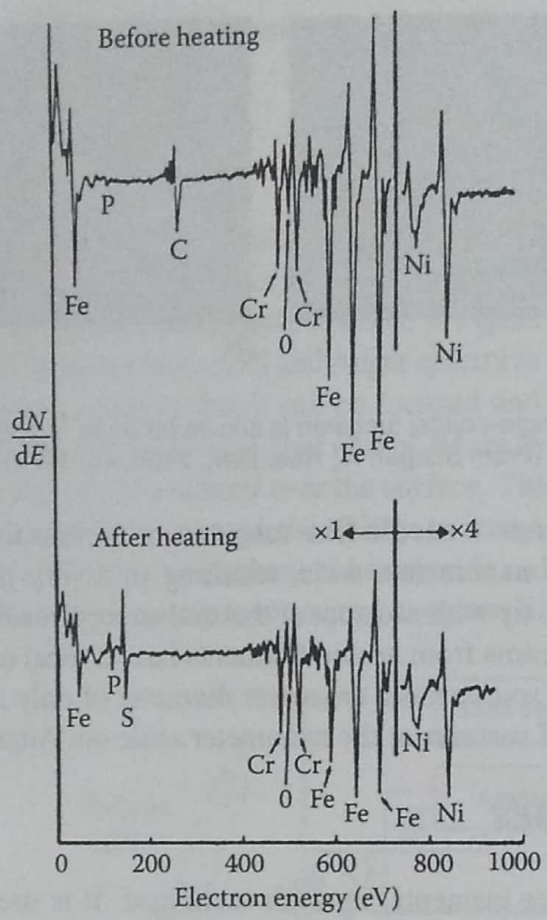

Figure 14.29 Auger spectra of stainless steel before and after heating in vacuum at 750°C for 10 min. As a result of heating, carbon has been lost from the surface while sulfur and phosphorus have diffused from the bulk steel to the surface.

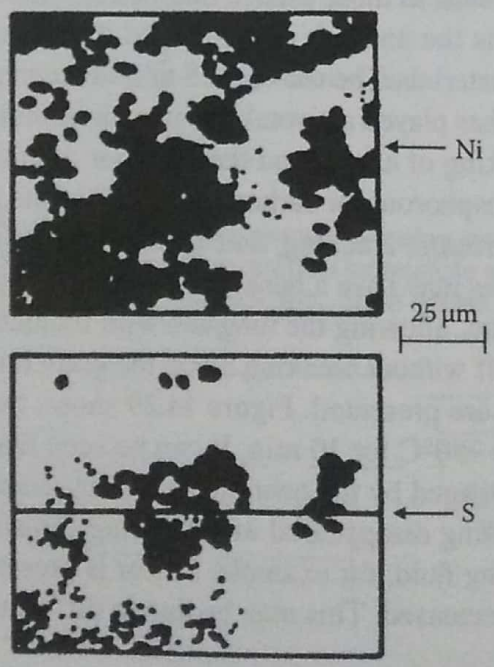

Figure 14.30 Auger element distribution maps of Ni and S on the surface of a spent catalyst, obtained by rastering the electron beam across the surface of the catalyst.

Figure 14.31 Auger element maps of an integrated circuit, showing the distribution of oxygen, gold, and molybdenum on the surface. (Courtesy of Physical Electronics, Inc., Eden Prairie, MN, www.phi.com.)

surface. In another example, Figure 14.31 shows the distribution of molybdenum, gold, and oxygen on an integrated circuit. Using this technique, it is possible to map the distributions of these three elements and their positions relative to the circuit. The use of a scanning mode and small spot size is called scanning Auger microscopy (or scanning Auger microprobe), known by the initials SAM.

14.2.2.2.1 Depth Profiling

As can be done with XPS, another valuable application of AES has been developed by using an ion beam to progressively strip off the surface of a sample under controlled conditions from a sample. Spectra can be collected and the distribution of elements recorded as surface material is removed. The results show changes in distribution of different elements with depth, called a depth profile.

A schematic diagram of a sample undergoing depth profiling is shown in Figure 14.32. The ion beam sputters the surface and etches a crater into the material, while the electron beam is used as the source for AES. Figure 14.33 shows the results of such a depth profile investigation of Nichrome film on a silicon substrate. It can be seen from the plot that the Nichrome film and its outer oxide layer are about 150–175 Å thick. That can be deduced from the appearance of the Si substrate after about 175 Å of material has been sputtered off. It is also evident that the chromium at the outer surface has formed an oxide layer about 75 Å thick. Chromium readily forms a protective oxide layer when exposed to air. The oxygen signal decreases after the oxide layer has been sputtered off, revealing the Ni and Cr film itself. Information about surface oxide layers, layer thickness, and composition is critical to understanding corrosion chemistry, surface reactions, material behavior, and device fabrication.

Another example of depth profiling is shown in Figure 14.34; AES clearly shows the very localized region containing Cl at a depth of about 1100 Å from the surface of the material.

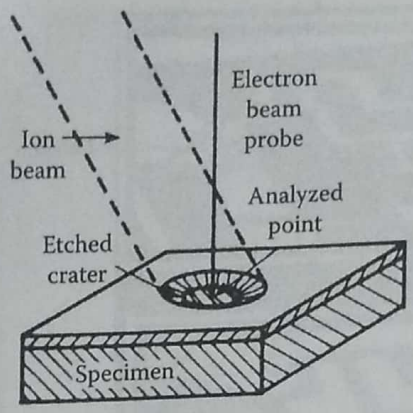

Figure 14.32 Use of ion sputtering for depth profile analysis. An ion gun is used to remove surface layers during collection of Auger spectra. (Courtesy of Physical Electronics, Inc., Eden Prairie, MN, www.phi.om.)

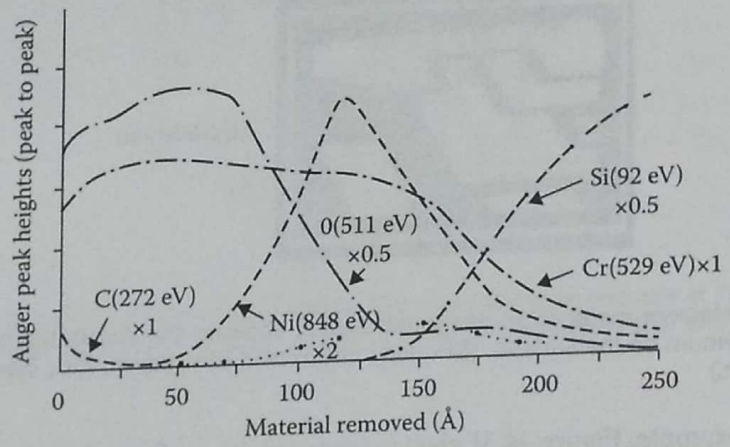

Figure 14.33 Depth profile analysis of a Nichrome film on a silicon substrate. The outermost layer shows both Cr and oxygen, probably as a stable chromium oxide layer. The Ni and Cr (the Nichrome film) signals drop off at about 175 Å while the Si substrate signal starts to appear, indicating the approximate film thickness. (From Weber, R.E., *Res. Dev.*, 10, 22, 1972.)

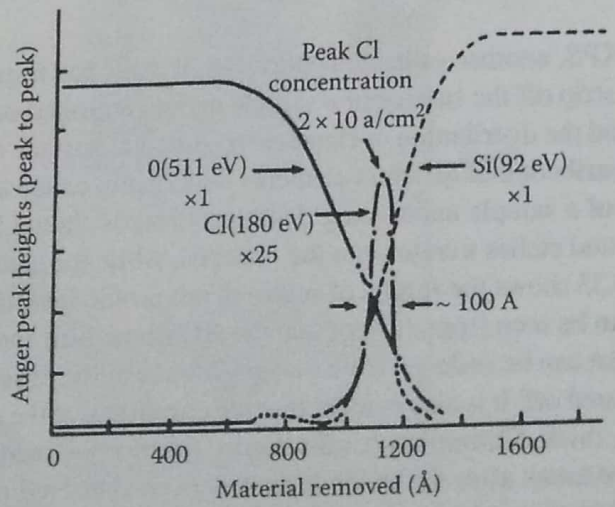

Figure 14.34 Depth profile of material with a highly localized narrow region containing Cl. The high lateral resolution of AES allows the characterization of thin layers and small features, such as this 100 Å thick Cl-containing region. (From Weber, R.E., *Res. Dev.*, 10, 22, 1972.)

The Cl-containing region is only about 100 Å wide. This extremely fine lateral resolution is one of the strengths of AES over other analytical techniques.